INTERNATIONAL ATOMIC ENERGY AGENCY
UNITED NATIONS EDUCATIONAL, SCIENTIFIC AND CULTURAL ORGANIZATION
INTERNATIONAL CENTRE FOR THEORETICAL PHYSICS
I.C.T.P., P.O. BOX 586, 34100 TRIESTE, ITALY, CABLE: CENTRATOM TRIESTE

SMR.780 - 26

FOURTH AUTUMN COURSE ON MATHEMATICAL ECOLOGY

(24 October - 11 November 1994)

"Self-organization of Front Patterns in Large Wildebeest Herds"

Simon A. Levin
Department of Ecology and Evolutionary Biology
Princeton University
Princeton, NJ 08544-1003
U.S.A.

These are preliminary lecture notes, intended only for distribution to participants.

3 copies

J. theor. Biol. (1993) **165**, 541–552

Self-organization of Front Patterns in Large Wildebeest Herds

SHAY GUERON† AND SIMON A. LEVIN‡

†*Center for Applied Mathematics, 504 ETC Building, Cornell University, Ithaca, NY 14853 and*
‡*Department of Ecology and Evolutionary Biology, Princeton University, 203 Eno Hall, Princeton, NJ 08544-1003, U.S.A.*

(*Received on 9 September 1992, Accepted in revised form on 19 February 1993*)

Aerial photographs of migrating wildebeest herds reveal striking distributional patterns, including wavy fronts. These patterns vary over scales that are much larger than the individual's perceptual range, and thus cannot be explained simply as random fluctuations on uniformity. Furthermore, since the individual is only aware of its immediate surroundings, broad-range patterns must be explained in terms of local decisions.

This paper suggests a model for the dynamics of large herds and a mechanism for their self-organizing pattern formation. We overcome the problem of modeling a two-dimensional distribution of a large population by considering only the leading layer. The conditions under which uniform fronts are stable (or unstable) are analyzed. In the latter case, small perturbations on uniformity evolve to large-scale patterns, as we demonstrate by computer simulations. We suggest this as a possible mechanism for spontaneous generation of long-range patterns.

1. Introduction

Wildebeest herds, massing in the Serengeti during migration season, are a spectacular sight. Aerial photographs of these herds reveal a striking variety of patterns formed by the herd's front (Sinclair, 1977; Scott, 1988). All share the same characteristic zigzagged irregular wavy front, with a typical wavelength large with respect to the body-length (e.g. see Fig. 1).

The absence of any evidence of long-range communication in the herd, means one must seek explanation of such patterns in terms of local interactions. The individual wildebeest lacks any knowledge about remote sections of the herd, and rather is aware only of its immediate surroundings. Yet, front patterns consistently vary over a scale much larger than the individual's perceptual range. Were this phenomenon the result of random fluctuations on uniformity, the typical wavelength would be much smaller (body-length scale) and the patterns would not be easily distinguishable by means of aerial photography. Consequently, one must assume that they are self-organizing, building and reinforcing on inhomogeneities. In this paper we seek the mechanisms responsible for spontaneous generation of such long-range patterns.

Grouping is a common social behavior in mammals. The number of individuals in herds can range from dozens (e.g. zebra) to hundreds [e.g. bison, buffalo

0022-5193/93/024541 + 12 $08.00/0

(Mloszewski, 1983)]. Perhaps the largest examples are wildebeest herds, which can consist of 100 000 individuals or more (Sinclair, 1977). Herding is probably a response to predation, decreasing the individual's chance of being preyed upon (Bertram, 1978).

Many models, both discrete and continuous, have been suggested to incorporate gregarious behavior in various species (see Okubo, 1986, for a review). In the continuous models (e.g. Keller & Segel, 1971; Odell & Keller, 1976; Gueron & Liron, 1989) the population is represented by a density function (i.e. number/amount of individuals per unit area) and the dynamics of the continuum is described by appropriate differential equations. The fundamental assumption underlying continuous models is that "many" individuals are found in an area whose characteristic dimension is small compared to the length scale of the pattern to be explained. While this assumption may be appropriate for insect swarms (e.g. Okubo & Chiang, 1974) or bacterial aggregations (e.g. Gueron & Liron, 1989), it is less suitable for most mammalian herds. The relatively small number of individuals (compared with bacterial populations, for example), the typical animal spacing (body-length scale) and the typical area occupied by the herd vitiate the continuum assumptions. In such cases, therefore, individual-based models, discrete in form, may be more appropriate. Such models consider a finite number of individuals, and the rules that control the group dynamics are based on a finite sequence of decisions, taken by each individual at each time step (e.g. Hamilton, 1971; Grünbaum, 1992; Huth & Wissel, 1992).

Obviously, one cannot seek to account for the behavior of every individual in a herd involving more than a few individuals, and some simplifications are necessary. These are justified by our recent simulations with small herds (Gueron *et al.*, unpublished data). For small herds we found that differences in the intrinsic walking speeds are enough to cause faster individuals ("speeders") to become "leaders" (i.e. the individuals at the front, with respect to the direction of propagation); consequently, we assume that leaders emerge from a distinct subgroup of the herd, characterized by intrinsic physical traits. Since the interesting patterns develop with the leaders, one can regard *only* the "leading band" for analyzing this phenomenon at the scale that the patterns are observed. This enables modeling of (the front of) a two-dimensional "array" of many individuals with the reduced computational effort of modeling a curve in two dimensions. With this simplification, we were able to model and simulate the leading-front band of wildebeest herds, as detailed in sections 2 and 3. The conditions that make traveling fronts stable or unstable are analyzed in section 4. For the unstable cases, small perturbations on uniformity evolve and form large-scale patterns, as revealed by the simulation results presented in section 5. We therefore suggest that long-range patterns can, indeed, arise spontaneously through the instability of uniform distributions, and subsequent enhancement due to local interactions.

2. Modeling Assumptions and Notations

For large aggregations, such as wildebeest herds, clearly one should not endeavor to account for the dynamics of every individual in the herd. One must strive either

FIG. 1. An aerial photograph of a large wildebeest herd, revealing the large-scale patterns discussed in the paper. Courtesy of A. R. E. Sinclair (plate 3, taken from his book *The African Buffalo*).

for stati
duals, or
problem"
To this
et al., un
i.e. the in
to a distin
walking p
distributio
finally ge
propagatio
simplificat
developme
band" for a
The front
time and s
directionali
the velocity
remains con
direction of
Individua
when they
interact, the
behavior pat
The intera
position with
operator

Δ is a mea
"leading", con
each side) surr
The (positive
is. In our pap
discussed front
modeled as a fu
($v_0(t)$) and the a
neighbors. A s
velocity ($\dot{y}$) as

for some (differe
the interaction.

3.

for statistical mechanics (Grünbaum, 1992), based on ensemble behavior of individuals, or for simplifications that reduce the prohibitive complexity of the "full problem".

To this end, we use the results of our recent simulations with small herds (Gueron *et al.*, unpublished data). Modeling of small herds revealed that the herd "leaders" (i.e. the individuals at the front, with respect to the direction of propagation) belong to a distinct group, namely those that (for whatever reason) inherently have a faster walking pace (speeders). Without any global plan (or knowledge of the global distribution of the herd), speeders simply advance, overtaking slower individuals, and finally generate a leading band that consists of only speedy individuals. The propagation direction is controlled mainly by these leaders. This allows for some simplifications in modeling wildebeest herds at large scales. Since the pattern development we are addressing is defined by the leaders, we regard *only* the "leading band" for analyzing this phenomenon.

The front layer is modeled as a curve $y(x, t)$, $x \in (-\infty, \infty)$, $t \geq 0$ evolving in both time and space. In this model we assume that the speedy band has "perfect directionality". This contributes a further simplification by implying that changes in the velocity are reflected only by changes in its magnitude (while the direction remains constant). With no loss of generality, this direction is chosen to be the direction of the Y axis.

Individuals are considered to have an inherent preferred speed at which they walk when they do not interact with their (left and right) neighbors. When they do interact, they adjust (increase or decrease) their speeds according to an intrinsic behavior pattern.

The interaction among the herd members is modeled as a function of the relative position with respect to the neighbors. The relative position is defined by the operator

$$\Delta(y(x, t)) = \frac{1}{2\delta} \int_{x-\delta}^{x+\delta} y(s, t)\, ds - y(x, t). \tag{1}$$

Δ is a measure of the extent to which an individual [located at the $y(x, t)$] is "leading", compared with the average location of the neighborhood (ranging δ to each side) surrounding it.

The (positive) parameter δ determines how local the interaction with the neighbors is. In our paper δ is small compared with the characteristic wavelength of the discussed front patterns. This accounts for a local influence range. The velocity (v) is modeled as a function of Δ. We postulate that an individual has an intrinsic velocity ($v_0(t)$) and the ability to speed up or slow down as a result of the interaction with its neighbors. A straightforward way to model such behavior is by expressing the velocity ($\dot{y}$) as

$$\dot{y} = v_0(t) + F(\Delta(y)) \tag{2}$$

for some (differentiable) function F, where F is the speed adjustment that depends on the interaction.

3. Traveling Front Solutions

We begin by seeking steady-state solutions that produce "wavy" front patterns and, in particular, vary over scales that are larger than $O(\delta)$ (in other words, a typical "wavelength" should remain finite when $\delta \to \infty$). This leads us to look for traveling front (TF) solutions, defined as solutions of eqn (2) that have the form

$$y = u_0(t) + f(x) \tag{3}$$

for some (smooth) functions $u_0(t)$ and $f(x)$. A traveling front is called uniform (UTF) if $f(x)$ is constant (independent of x). As we shall show, no such TF solutions have the desired properties; however, solutions that bifurcate from some of the TF solutions do seem to mimic desired patterns.

In order to find the possible TF solutions we substitute the TF solution (3) into eqn (2) to obtain

$$\dot{u}_0(t) = v_0(t) + F(\Delta(f(x))). \tag{4}$$

Therefore, a necessary condition for a TF to exist is

$$F(\Delta(f(x))) = \text{const}, \tag{5}$$

which yields (assuming a non-trivial function F)

$$\Delta(f(x)) = \text{const}. \tag{6}$$

It is easy to see that condition (6) is also a sufficient condition for the existence of a TF; and if it is satisfied, u_0 can be computed so as to satisfy eqn (2).

The general solution of eqn (6) can be found if we restrict our discussion to solutions of polynomial order (i.e. solutions that are bounded by $c|x|^n$ as $|x| \to \infty$, for some positive integer n and a real constant c). Differentiating eqn (6) yields the differential difference equation

$$\frac{1}{2\delta}(f(x+\delta) - f(x-\delta)) = f'(x). \tag{7}$$

With the above restriction, the solutions of eqn (7) can be expressed as linear combinations of functions of the type

$$f(x) = p(x)\, e^{i\beta x}, \tag{8}$$

where β is a root of the characteristic equation of eqn (7) and $p(x)$ is a polynomial whose degree is less than the multiplicity of β as a root (Bellman, 1963). Simple computations show that this is equivalent to finding the real roots of the characteristic equation

$$\sin(\beta\delta) - \beta\delta = 0. \tag{9}$$

The only real solution of eqn (9) is $\beta = 0$, and its multiplicity is 3. Therefore, any quadratic

$$f(x) = Ax^2 + Bx + C \tag{10}$$

is a possible TF.

These solutions, however, are not bounded (for $A \neq 0$ or $B \neq 0$) on $x \in (-\infty, \infty)$, and do not yield the multiple peaks we seek.

4. Stability Analysis of Traveling Fronts

Looking at the front patterns of large herds (Fig. 1), one can clearly detect irregular "fingers" emerging in the propagation direction. None of the TF solutions described above exhibit such large-scale patterns, and thus we direct our efforts to stability properties of TF solutions. Let u be a TF solution of eqn (2). Assume that

$$\Delta(u(x)) = c_0 \tag{11}$$

[see eqn (6)] and that

$$F'(c_0) = b \neq 0. \tag{12}$$

The traveling front u is a (linearly) stable solution of eqn (2) if $b > 0$, and unstable if $b < 0$. For $0 < k < 1$ the TF u is always unstable.

To see this, consider a *small* perturbation (h) on the TF (u), namely

$$y = u(x, t) + h(x, t). \tag{13}$$

Differentiating eqn (2), with respect to x, and linearizing about $\Delta(u) = c_1$ yields

$$h_x = b\Delta(h) = \frac{b}{2\delta}[h(x+\delta, t) - h(x-\delta, t)] - bh_x. \tag{14}$$

We look for the modes [i.e. solutions of the differential–difference eqn (14)] that exhibit exponential behavior in time. These are defined as

$$h = e^{\alpha t} g(x) \tag{15}$$

for some function $g(x)$. If all of the possible values of α satisfy $Re(\alpha) < 0$, h decays exponentially, and the TF is stable. If there is a mode for which $Re(\alpha) > 0$, then h grows exponentially; and thus the UTF is considered unstable. The UTF is termed neutrally stable if it is not unstable, but there is a mode for which $Re(\alpha) = 0$.

Substituting the expression (15) into eqn (14) yields

$$\alpha g' = \frac{b}{2\delta}[g(x+\delta) - g(x-\delta)] - bg'. \tag{16}$$

The (polynomial order) solutions of this difference equation are exponentials of the type $g(x) = e^{i\mu x}$. Since $g(x)$ is the perturbation at that time $t = 0$ [see eqn (15)], it must be bounded on $x \in (-\infty, \infty)$, to avoid violating the assumption that h is a small perturbation on u. This implies that μ must be real.

Equation (16) gives

$$(\alpha + k)i\mu = \frac{b}{2\delta}[e^{i\mu\delta} - e^{-i\mu\delta}] = \frac{ib}{\delta}\sin(\mu\delta) \tag{17}$$

and finally translates to

$$\alpha = b\left(\frac{\sin(\mu\delta)}{\mu\delta} - 1\right). \tag{18}$$

The conclusion is that the signs of α and b are opposite, which completes the proof.

We can now apply the stability analysis to the only bounded solution in this case, namely, the UTF [i.e. $A = B = 0$, $C \neq 0$ in eqn (10)]. With $\Delta(\text{const}) = 0$, F becomes the response to deviations from uniformity. With no loss of generality we assume that $F(0) = 0$, which allows v_0 to be interpreted as the walking speed when "leveled up" with the neighbors.

The case where $b > 0$ implies that trailers speed up and leaders slow down. With this interpretation it is clear that UTF is a stable solution that would evolve from arbitrary initial conditions. In the case $b < 0$, leaders are "encouraged" by being ahead of the local surroundings and tend to speed up so as to maintain this situation. The trailers do the opposite. With this behavior pattern the UTF is unstable. This instability may potentially yield the desired patterns (the behavior of the unstable solutions will be demonstrated in the Results).

The value of μ that maximizes α for the case $b < 0$, that is of interest because it gives a rough approximation to the characteristic wavelength observed with the nonlinear problem, is considered. Computing this value from eqn (18) yields

$$\mu_{\max} \sim \frac{4{\cdot}493}{\delta}. \tag{19}$$

5. Results

For numerical computations, eqn (2) is transformed to the discrete form

$$\dot{y}_i = v_0(t) + F(\Delta(y_i)), \quad i = 1 \ldots n \tag{20}$$

and Δ is replaced with

$$\Delta(y_i(x, t)) = \frac{1}{2p+1} \sum_{j=i-p}^{i+p} y_j - y_i. \tag{21}$$

The continuous (infinite) region $x \in (-\infty, \infty)$ is replaced with the finite set of samples at $i = 1 \ldots n$. In order to simulate an "infinite" curve (and overcome the definition problem at the indices $n-p < j \leq n$ and at $0 < j < p$), we define the running index (j) in eqn (21) above, in a "wrap around" order [i.e. $j \equiv j \bmod n$, for $n-p < j < n$ and $j \equiv n + (j \bmod n)$ for $0 < j \leq p$].

Equations (20) and (21) form a system of n coupled ordinary differential equations for the variables y_i.

$y_i(t)$ represents a segment of the herd's front layer. The interpretation we give the discrete description is that the front-layer segment is represented by n "pixels". The distance between two neighboring pixels is defined as one unit. At the scale we observe the herd, each pixel may be a cluster of several individuals. The rest of the herd (i.e. the trailing layers), which is not modeled explicitly, lies behind the front layer (in the negative direction of the Y axis) and "fills in the gaps" as they develop. From eqn (21) it follows that each pixel interacts with p neighbors (on each side). Local interaction is implemented by satisfying $p/n \ll 1$.

Equations (20) and (21) are written in dimensionless form. We define our length

and time units in such a way that the intrinsic velocity, v_0, equals 1. In the simulations, we chose a dimensionless time step of 0·1.

F, the response to displacement from a uniform position, satisfies $F(0) = 0$. It should also be bounded. Since it represents the velocity change, corresponding to a given displacement, its magnitude should not exceed v_0 (to avoid negative velocities, or exceeding twice the intrinsic velocity). F should have one positive and one negative simple root. This ensures that when the magnitude of displacement is too large, the behavior trend is reversed, which is important to keep the herd from segregating (otherwise, for example, encouraged speeders will go on speeding and never stop to "wait" for the trailers to catch up). For our simulations we used a particular function that satisfies the above requirements, namely

$$F(\Delta) = \pm \sin(\Delta), \tag{22}$$

where the sign $\pm$ is chosen as $+$ to demonstrate the stable cases (i.e. cases where the uniform traveling front is a stable solution) and for the unstable cases (cases where the uniform traveling front is an unstable solution).

For the stable case, the response to lagging behind is speeding up, and the response to being ahead is slowing down. As implied by the stability analysis, the uniform traveling front is a stable solution for such cases. It is expected to be an "attractor" in the sense that any initial conditions will eventually lead to a uniform front after a long enough time has elapsed. This was, indeed, the case in all of the "stable" models' simulations. As an example we present the results of a run with $n = 250$ and $p = 2$. The initial arrangement was the randomly perturbed wave (containing six cycles)

$$y_i(0) = 5\left(\sin\left(\frac{6\pi i}{n}\right) + \sin\left(\frac{12\pi i}{n}\right) + R_i\right), \tag{23}$$

where $-0{\cdot}2 \le R_i \le 0{\cdot}2$ is a random perturbation.

Figure 2 shows plotted traces of $y_i(t)$ versus i for different time steps. Clearly, the initial pattern decays to a uniform front.

In the unstable cases, the response to lagging behind is slowing down (until the gap reaches the saturation level where the behavior is reversed). On the other hand, being ahead is "encouraged" by speeding up (until the gap reaches the saturation level where the behavior is reversed). For such cases the uniform front is an unstable solution, and small perturbations are expected to grow and to generate some irregular patterns. Our main goal was to check whether the unstable case can yield "wavy" fronts where the typical wavelength is on a larger scale than the typical interaction range. This was found to be true, and "local" rules produced "long range" effects. We also found that, after bifurcating from the uniform arrangement, these solutions reach a "semi-steady state"; although they keep changing (in time), the changes remain on a small scale and thus the global patterns seem persistent. One of the factors that controls that actual "shape" of the generated patterns is how local the interaction range is (i.e. p). To demonstrate these observations we present the

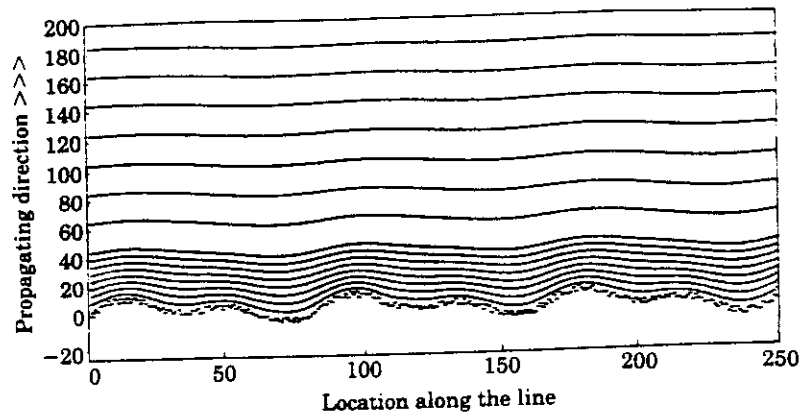

FIG. 2. The stable case. Traces of $y_i(t)$ versus i for 17 different time steps $t = 0, 50, 100, 150, 200, 250, 300, 350, 400, 600, 800, 1000, 1200, 1400, 1600, 1800, 2000$.

results of three runs with $n = 1000$ and $p = 1, 2, 3$, respectively. The initial conditions were set as

$$y_i(0) = 0{\cdot}1\left(\sin\left(\frac{\pi i}{2n}\right) + \sin\left(\frac{\pi i}{n}\right) + R_i\right). \tag{24}$$

The results are displayed in Figs 3–5. These are plots of $y_i(t)$ versus i (for $t = 200$) with shaded areas that represent the trailing layers as they "fill in the gaps". The shaded areas were added to the plots, to make the results easy to be compared with aerial photographs of actual wildebeest herds. The qualitative agreement is, indeed, satisfactory (see Fig. 1). Further, comparing Figs 3, 4 and 5, which represent simulations with different values of δ, reveals that the ratio of the observed characteristic wavelengths is roughly as predicted from eqn (19).

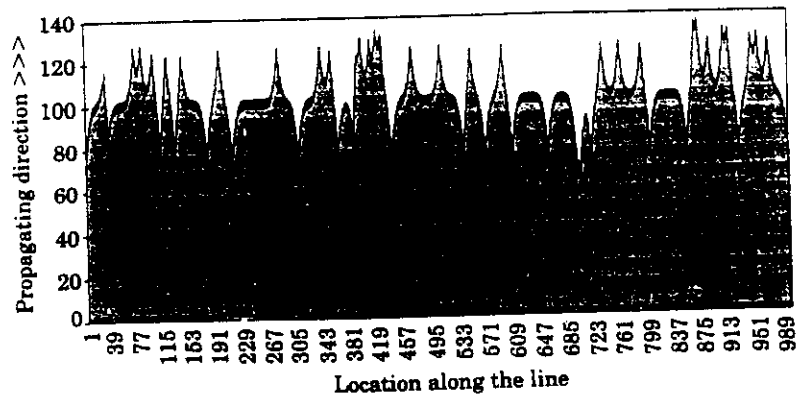

FIG. 3. The unstable case. Traces of $y_i(t = 2000)$ versus i with shaded areas that represent the trailing layers as they "fill in the gaps". In this run $p = 1$. The smooth initial conditions produce wavy patterns.

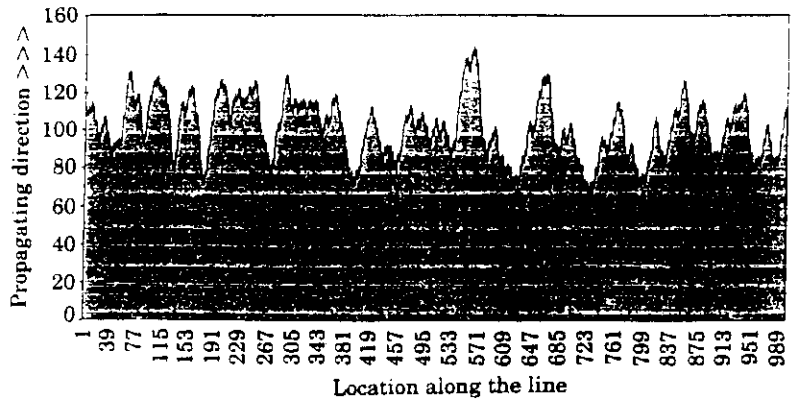

FIG. 4. The unstable case. Traces of $y_i(t = 2000)$ versus i with shaded areas that represent the trailing layers as they fill in the gaps. In this run $p = 2$. The smooth initial conditions produce wavy patterns.

In order to compare the qualitative properties of the different fronts and their dependence on n and p, we define the "effective length" (EL) as the length of the curve (defined by the front), divided by n. With this definition, the EL of a uniform front is 1, and larger EL values indicate more "oscillatory" patterns.

Since different values of n correspond to modeling different front segment-sizes, it is important to verify first that the EL is independent of n. If this were not the case, it would mean that the fronts have a fractal dimension different from one, and any observations might depend on the discussed front-segment (i.e. the number of pixels that are considered) rather than only on the intrinsic parameters of the model. In Fig. 6 we display the dependence of the EL on n for $p = 1, 2, 3$ (with the unstable case). It is shown that the EL is independent of n, which indicates that modeling a 1000-pixel front is a sufficient basis to draw conclusions.

From Fig. 6 one can also conclude that the EL is a decreasing function of p. This is

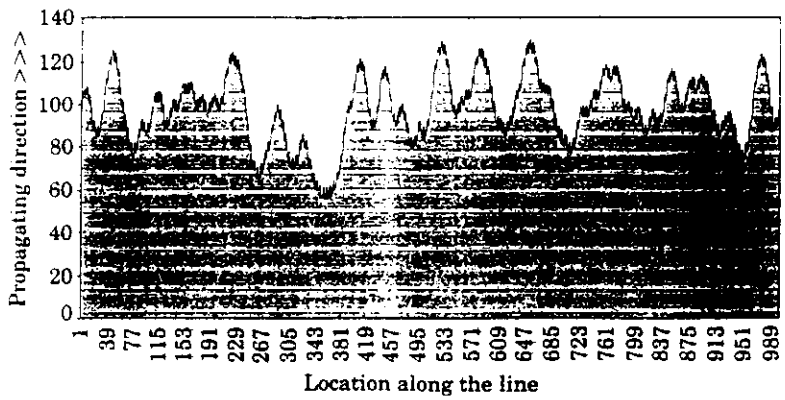

FIG. 5. The unstable case. Traces of $y_i(t = 2000)$ versus i with shaded areas that represent the trailing layers as they fill in the gaps. In this run $p = 3$. The smooth initial conditions produce wavy patterns.

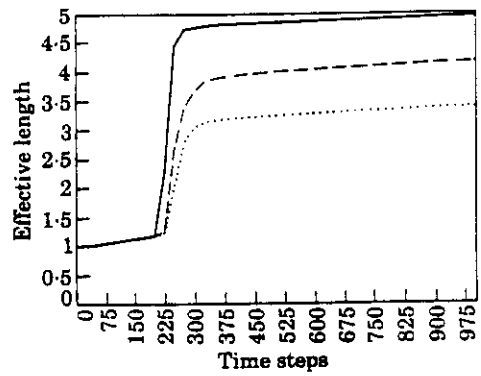

FIG. 6. The dependence of the front effective length on the number of pixels (n), for the unstable case, for three values of p, measured at $t = 1000$. (——), one interacting neighbor; (– – –), two interacting neighbors; (····), three interacting neighbors.

emphasized even more in Fig. 7 that shows the dependence of the EL on p, for $n = 1000$. It implies that the fronts become more "erratic" as the interaction becomes more local.

Figure 8 displays the dependence of the EL on the elapsed time. The EL reaches an asymptotic value (depending on the different values of p) after ~ 400 time steps. This indicates that pattern generation is a persistent phenomenon. A relatively short time (less than 15 time steps) after the fronts start evolving, they attain their final characteristics, which are maintained thereafter.

6. Discussion

The aim of the model was to suggest a mechanism for self-organizing front patterns. This addresses a basic question in pattern formation: how can a long range effect emerge from very local mechanisms? Our model suggests a simple mechanism

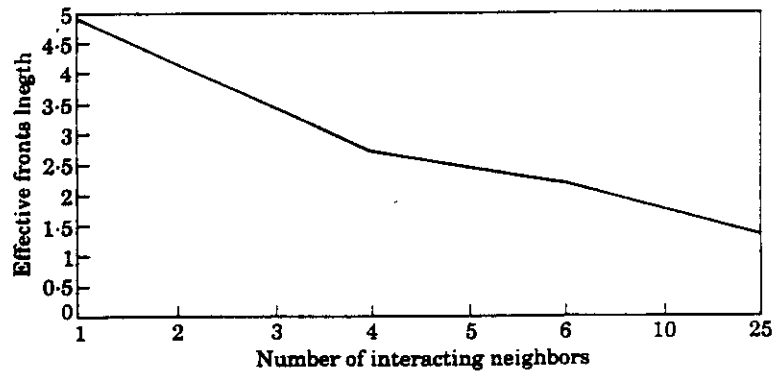

FIG. 7. The dependence of the front effective length on the number of interacting pixels (p) for the unstable case. Here, $n = 1000$ and the EL are measured at $t = 1000$.

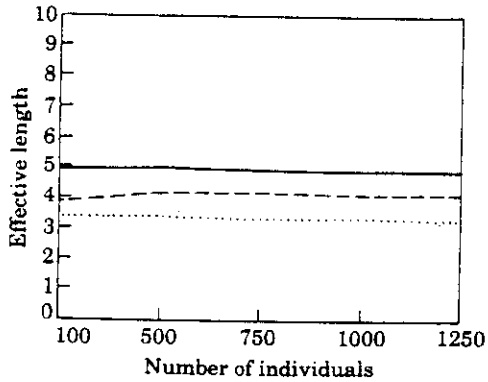

FIG. 8. The time dependence of the front effective length, for $n = 1000$ and three values of p. (——), one interacting neighbor; (— — —), two interacting neighbors; (· · · ·), three interacting neighbors.

that spontaneously produces the front patterns, namely, the instability of a traveling front.

The reason we deal with traveling front solutions and then investigate the patterns that bifurcate from traveling fronts (as an instability effect), is the persistent appearance of the fronts in different aerial photographs. This indicates that we cannot rely on transients to explain these frequent occurrences. The results we obtain from the unstable cases show characteristic resemblance to the experimental evidence. These evolving fronts also have the important property of persisting for long time periods, thus making them easily noticeable phenomena, as required. Of great interest is the fact that the patterns fit the experimental observations better as the neighbor interaction becomes more local. Further, simulations done with large values of p (e.g. more than 10) yield flatter fronts. Whereas the individual cannot be expected to have a long perceptual range, it is certainly reasonable to assume that it could adjust its behavior according to its nearest neighbors.

We conclude with pointing out another application of our approach for modeling narrow bands of walking animals, such as commonly observed winding lines (two or three individuals in width) of wildebeest, zebra or buffalo (e.g. Sinclair, 1977; Scott, 1988), or ant trails (Wilson, 1971; Alt & Hoffmann, 1990). The analysis offered in the previous sections can be applied to such problems as well, in order to explain the generation of the wavy patterns defined by these bands. For this, one can assume that the propagation is in the direction of the x axis and that (in this direction) the individuals keep the same spacing from each other. In addition to marching in the x axis direction, an individual can adjust its position compared with its (back and front) neighbors by moving sideways. In cases where only the front neighbors are considered, the operator Δ [eqn (1)] should be defined as "one sided". With the modified interpretation, v_0 should equal 0 in eqn (2) (i.e. no translation in the y direction). The rest of the analysis remains as it is.

The research of S. Gueron was supported by the Cornell University Center for Applied Mathematics and the Theory Center, and partly by a Rothschild Fellowship. The research of

S. Levin was supported by NSF grant DMS 9108195 and by the Office of Naval Research through its URIP initiative to Woods Hole Oceanographic Institution. We thank Joy Belsky, John Guckenheimer, Nadav Liron and Dan Rubenstein for insightful discussions and suggestions.

REFERENCES

ALT, W. & HOFFMANN, G. (eds). (1990). Biological motion. *Lecture Notes in Biomathematics*, 89. Berlin: Springer-Verlag.

BELLMAN, R. E. (1963). *Differential-Difference Equations*. New York: Academic Press.

BERTRAM, B. (1978). *Behavioral Ecology*. Sunderland, MA: Sinauer Associates.

GUERON, S. & LIRON, N. (1989). A model of herd grazing as a travelling wave, chemotaxis and stability. *J. math. Biol.* **27**, 595–608.

GRÜNBAUM, D. (1992). Aggregation models of individuals seeking a target density, Ph.D. thesis, Ithaca, NY, Cornell University.

HAMILTON, W. D. (1971). Geometry for the selfish herd. *J. theor. Biol.* **31**, 295–311.

HUTH, A. & WISSEL, C. (1992). The simulation of movement of fish schools. *J. theor. Biol.* **156**, 365–385.

KELLER, E. & SEGEL, L. (1971). Travelling bands of chemotactic bacteria: A theoretical analysis. *J. theor. Biol.* **30**, 235–248.

MLOSZEWSKI, M. J. (1983). *The Behavior and Ecology of the African Buffalo*. New York: Cambridge University Press.

ODELL, G. & KELLER, E. (1976). Travelling bands of chemotactic bacteria revisited. *J. theor. Biol.* **56**, 243–247.

OKUBO, A. (1986). Dynamical aspects of animal grouping: swarms, schools, flocks and herds. *Adv. Biophys.* **22**, 1–94.

OKUBO, A. & CHIANG, H. C. (1974). An analysis of the kinematics of swarming of *Anarete pritchardi* Kim (Diptera: Cecidomyiidae). *Res. Popul. Ecol.* **16**, 1–42.

SCOTT, J. (1988). *The Great Migration*. Emmaus, PA: Rodale Press.

SINCLAIR, A. R. E. (1977). *The African Buffalo, A Study of Resource Limitation of Population*. Chicago, IL: The University of Chicago Press.

WILSON, E. O. (1971). *The Insect Societies*. Cambridge, MA: Belknap Press of Harvard University Press.